Thiol-Linked Anthraquinone Anthryl Acetylene Molecule: Synthesis, Self-assembly, and Photoelectrochemical Properties

Hong Ma, Mun-Sik Kang, Qing-Min Xu, Kyoung-Soo Kim, and Alex K.-Y. Jen*

Department of Materials Science and Engineering, University of Washington, Seattle, Washington 98185-2120

Received February 1, 2005. Revised Manuscript Received April 11, 2005

A novel self-assembling molecule with coplanar anthraquinonyl and anthryl moieties linked by an acetylenic unit has been designed and synthesized as an electron acceptor for efficient photocurrent generation. The high-resolution scanning tunneling microscopy (STM) images showed that the self-assembled monolayer (SAM) of this molecule forms highly ordered two-dimensional (2D) arrays on Au(111) with an oblique lattice and graphite-like stacking at room temperature. The electrochemical study of this molecule and its SAM on Au showed reversible characteristics. The SAMs generated by co-assembling this acceptor with an oligo(pyrrolethiophene) donor show very promising photoelectrochemical properties. The amount of photocurrent generated (up to 1425 nA/cm^2, 23.1% of quantum yield) under the illumination of 360 nm light is comparable to that obtained from using a C_{60}-based molecule as the electron acceptor (1700 nA/cm^2). This result demonstrates the feasibility of using anthraquinone-anthrylacetylene-thiol linked molecule as an efficient electron acceptor for constructing a monochromatic light-to-current molecular converter.

Introduction

Inspired by very efficient conversion of solar energy into chemical potential in photosynthesis, extensive efforts have been spent to systematically organize light-harvesting groups, electron donors, and electron acceptors at the molecular level to mimic the natural systems.[1] Many synthetic diads, triads, and even pentads that contain porphyrins or oligothiophenes as donors and quinone, C_{60}, or peryleneimide as acceptors have been investigated for their efficiency in light-harvesting, energy transfer, electron transfer, or charge separation which are all the important processes for photosynthesis.[2−4] However, it remains a very challenging task to combine all of this knowledge to create a system that can efficiently convert photons to electrons. To mimic the highly organized and elaborate molecular machinery of natural systems, several strategies for the construction of artificial photosynthetic systems by arranging molecules in order through lipid bilayer membranes,[5] Langmuir−Blodgett (LB) films,[6] or self-assembled monolayers (SAMs), have been attempted.[7] Due to the relatively stable, uniform, well-packed, and two-dimensional structures that can be formed by SAMs,[8] a number of C_{60}-,[9] semiconductor nanoparticle-,[10] and metal complex-based[11] SAMs have been explored recently and

* To whom correspondence should be addressed. E-mail: ajen@u.washington.edu.

(1) (a) Guldi, D. M. *Chem. Soc. Rev.* **2002**, *31*, 22. (b) Gust, D.; Moore, T. A.; Moore, A. L. *Acc. Chem. Res.* **2001**, *34*, 40. (c) Wasielewski, M. R. *Chem. Rev.* **1992**, *92*, 435. (d) Deisenhofer, J., Norris, J. R., Eds. *The Photosynthetic Reaction Center*; Academic Press: New York, 1993.

(2) (a) Fukuzumi, S.; Okamoto, K.; Yoshida, Y.; Imahori, H.; Araki, Y.; Ito, O. *J. Am. Chem. Soc.* **2003**, *125*, 1007. (b) Samorì, P.; Yin, X.; Tchebotareva, N.; Wang, Z.; Pakula, T.; Jäckel, F.; Watson, M. D.; Venturini, A.; Müllen, K.; Rabe, J. P. *J. Am. Chem. Soc.* **2004**, *126*, 3567. (c) Tkachenko, N. V.; Tauber, A. Y.; Hynninen, P. H.; Sharonov, A. Y.; Lemmetyinen, H. *J. Phys. Chem. A* **1999**, *103*, 3657. (d) Rubtsov, I. V.; Kang, Y. K.; Redmore, N. P.; Allen, R. M.; Zheng, J.; Beratan, D. N.; Therien, M. J. *J. Am. Chem. Soc.* **2004**, *126*, 5022. (e) Gouloumis, A.; Liu, S. G.; Vázquez, P.; Echegoyen, L.; Torres, T. *Chem. Commun.* **2001**, 399.

(3) (a) Schuster, D. I.; Cheng, P.; Jarowski, P. D.; Guldi, D. M.; Luo, C.; Echegoyen, L.; Pyo, S.; Holzwarth, A. R.; Braslavsky, S. E.; Williams, R. M.; Klihm, G. *J. Am. Chem. Soc.* **2004**, *126*, 7257. (b) Ohkubo, K.; Kotani, H.; Shao, J.; Ou, Z.; Kadish, K. M.; Li, G.; Pandey, R. K.; Fujitsuka, M.; Ito, O.; Imahori, H.; Fukuzumi, S. *Angew. Chem., Int. Ed.* **2004**, *43*, 853. (c) Giacalone, F.; Segura, J. L.; Martín, N.; Guldi, D. M. *J. Am. Chem. Soc.* **2004**, *126*, 5340. (d) Pan, J.; Xu, Y.; Sun, L.; Sundström, V.; Polívka, T. *J. Am. Chem. Soc.* **2004**, *126*, 3066. (e) Choi, M. S.; Aida, T.; Luo, H.; Araki, Y.; Ito, O. *Angew. Chem., Int. Ed.* **2003**, *42*, 4060.

(4) (a) Weiss, E. A.; Ahrens, M. J.; Sinks, L. E.; Gusev, A. V.; Ratner, M. A.; Wasielewski, M. R. *J. Am. Chem. Soc.* **2004**, *126*, 5577. (b) Neuteboom, E. E.; Meskers, S. C. J.; van Hal, P. A.; van Duren, J. K. J.; Meijer, E. W.; Janssen, R. A. J.; Dupin, H.; Pourtois, G.; Cornil, J.; Lazzaroni, R.; Brédas, J. L.; Beljonne, D. *J. Am. Chem. Soc.* **2003**, *125*, 8625.

(5) (a) Komatsu, T.; Moritake, M.; Tsuchida, E. *Chem. Eur. J.* **2003**, *9*, 4626. (b) Seta, P.; Bienvenue, E.; Moore, A. L.; Mathis, P.; Bensaaaon, R. V.; Liddell, P.; Pessiki, P. J.; Joy, A.; Moore, T. A. *Nature* **1985**, *316*, 653.

(6) (a) Chen, J.; Mitsuishi, M.; Aoki, A.; Miyashita, T. *Chem. Commun.* **2002**, 2856. (b) Fujihira, M. *Mol. Cryst. Liq. Cryst.* **1990**, *183*, 59.

(7) (a) Uosaki, K.; Kondo, T.; Zhang, X. Q.; Yanagida, M. *J. Am. Chem. Soc.* **1997**, *119*, 8367. (b) Imahori, H.; Fukuzumi, S. *Adv. Func. Mater.* **2004**, *14*, 525. (c) Yasutomi, S.; Morita, T.; Imanishi, Y.; Kimura, S. *Science* **2004**, *304*, 1944. (d) Ma, H.; Jen, A. K. Y. *The Spectrum* **2004**, *17* (3), 24.

(8) (a) Ulman, A., Ed. *Self-assembled Monolayers of Thiols*; Academic Press: San Diego, 1998. (b) Ulman, A. *Chem. Rev.* **1996**, *96*, 1533. (c) Bishop, A. R.; Nuzzo, R. G. *Curr. Opin. Colloid Interface Sci.* **1996**, *1*, 127. (d) Schreiber, F. *Prog. Sur. Sci.* **2000**, *65*, 151. (e) Mrksich, M.; Whitesides, G. M. *Annu. Rev. Biophys. Biomol. Struct.* **1996**, *25*, 55.

(9) (a) Yamada, H.; Imahori, H.; Nishimura, Y.; Yamazaki, I.; Ahn, T. K.; Kim, S. K.; Kim, D.; Fukuzumi, S. *J. Am. Chem. Soc.* **2003**, *125*, 9129. (b) Hirayama, D.; Takimiya, K.; Aso, Y.; Otsubo, T.; Hasobe, T.; Yamada, H.; Imahori, H.; Fukuzumi, S.; Sakata, Y. *J. Am. Chem. Soc.* **2002**, *124*, 532. (c) Imahori, H.; Norieda, H.; Yamada, H.; Nishimura, Y.; Yamazaki, I.; Sakata, Y.; Fukuzumi, S. *J. Am. Chem. Soc.* **2001**, *123*, 100. (d) Kim, K. S.; Kang, M. S.; Ma, H.; Jen, A. K. Y. *Chem. Mater.* **2004**, *16*, 5058.

10.1021/cm050243w CCC: $30.25
Published on Web 05/07/2005

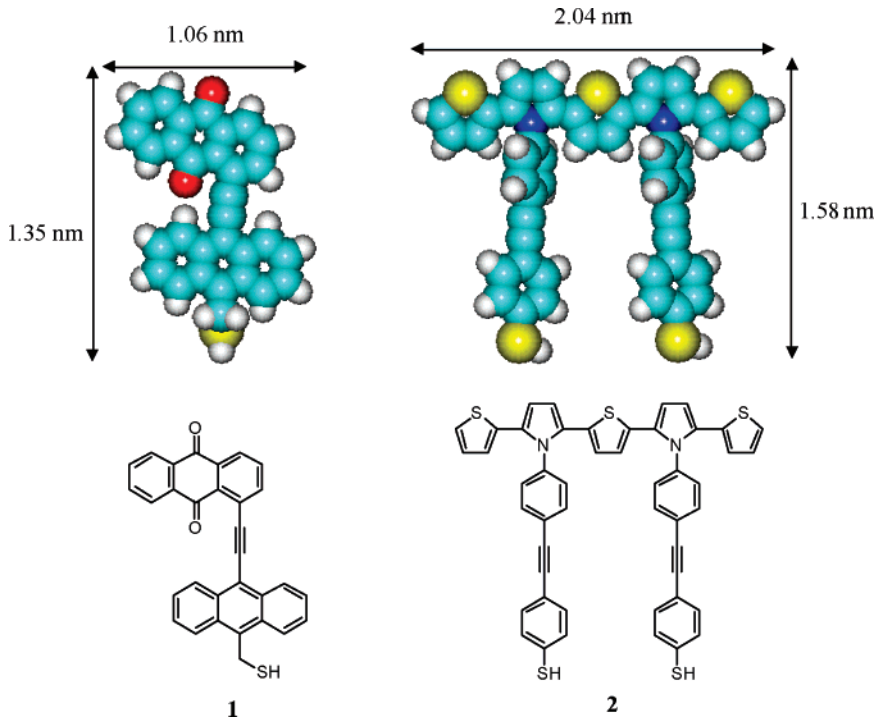

Figure 1. Schematic illustrations of self-assembling electron acceptor **1** and electron donor **2**. The structures were built by Hyperchem software and optimized by the AM1 method. The results from the AM1 calculation of molecule **1** show several kinds of stable (quasi-isoenergetic) conformations, but the molecule with a coplanar conformation forms the most stable SAM (further explanation can be seen in the Supporting Information).

shown to exhibit promising photocurrent generation. In nature, quinone and its derivatives play a very important role as electron acceptors in photosynthetic reactions and their reversible redox behavior in solution and SAMs have also been well-studied.[12] However, there is rarely any report regarding the use of quinone-based SAMs for photocurrent generation. Here, we describe the design, synthesis, ordered self-assembly, and photoelectrochemical properties of a conjugated anthraquinone derivative.

The performance of a functionalized SAM for photocurrent generation strongly relies on its structure, order, and packing density due to the influence of unidirectional electron transfer. Therefore, it is essential to design functional molecules capable of forming well-defined and ordered self-assemblies. In our earlier work we demonstrated the use of anthrylphenylacetylene thiols to form stable and ordered self-assemblies on Au(111) surface. These molecules tend to form highly ordered two-dimensional (2D) stacked arrays through the interplay of strong $\pi-\pi$ intermolecular stacking and chemisorptive gold−thiol interactions.[13a,b] Thus, by combining the electrochemically reversible properties of anthraquinone and the controllable nanoscale ordering provided by the anthrylphenylacetylene-based SAMs, we have designed and synthesized an efficient acceptor molecule, (10-(1-anthraquinonyl)acetylene)-9-anthrylmethylthiol (**1**) (Figure 1), to investigate its self-assembling characteristics and the photocurrent generation efficiency of its co-assembly with an oligo(pyrrolethiophene) donor molecule under the illumination of a monochromatic light. The anthraquinonyl moiety on top of **1** functions both as electron acceptor and a good modality for self-assembly due to its flat geometry for better $\pi-\pi$ interactions. Because of the linear and rigid acetylene spacer, it can prevent steric hindrance between the anthraquinone moiety and the underneath anthryl group to maintain coplanarity for better conjugation. This kind of molecular arrangement will also enhance the formation of ordered SAM and facilitate vectorial electron transfer.

Experimental Section

All chemicals were purchased from Aldrich and used as received unless otherwise specified. Tetrahydrofuran (THF) was distilled under nitrogen from sodium with benzophenone as the indicator. ^{1}H and ^{13}C NMR spectra were recorded on a Bruker-300 FT NMR (300 MHz) spectrometer with tetramethylsilane (TMS) as internal reference. Electrospray ionization mass spectra (ESI-MS) were obtained on a Bruker Daltonics Esquire Ion Trap Mass Spectrometer. Elemental analysis was determined at QTI (Whitehouse, NJ).

Synthesis of 1-Iodoanthraquinone (4). To the suspension of 1-aminoanthraquinone (**3**) (4.46 g, 20.0 mmol) in water (82 mL) and concentrated hydrochloric acid (14 mL) was added dropwise the solution of sodium nitrite (1.45 g, 21.0 mmol) in water (2.6 mL) at 0 °C under nitrogen. After the reaction mixture was

(10) (a) Sheeney-Haj-Ichia, L.; Wasserman, J.; Willner, I. *Adv. Mater.* **2002**, *14*, 1323. (b) Ogawa, S.; Hu, K.; Fan, F. F.; Bard, A. J. *J. Phys. Chem. B* **1997**, *101*, 5707.

(11) (a) Soto, E.; MacDonald, J. C.; Cooper, C. G. F.; McGimpsey, W. G. *J. Am. Chem. Soc.* **2003**, *125*, 2838. (b) Abdelrazzaq, F. B.; Kwong, R. C.; Thompson, M. E. *J. Am. Chem. Soc.* **2002**, *124*, 4796.

(12) (a) Long, Y. T.; Herrwerth, S.; Eck, W.; Grunze, M. *Phys. Chem. Chem. Phys.* **2002**, *4*, 522. (b) O'Hanlon, D.; Forster, R. J. *Langmuir* **2000**, *16*, 702. (c) Yoshimoto, S.; Hirakawa, N.; Nishiyama, K.; Taniguchi, I. *Langmuir* **2000**, *16*, 4399. (d) Ingram, R. S.; Murray, R. W. *Langmuir* **1998**, *14*, 4115. (e) Kondo, T.; Yanagida, M.; Nomura, S.; Ito, T.; Uosaki, K. *J. Electroanal. Chem.* **1997**, *438*, 121. (f) Zhang, L.; Lu, T.; Gokel, G. W.; Kaifer, A. E. *Langmuir* **1993**, *9*, 786. (g) Hickman, J. J.; Ofer, D.; Laibinis, P. E.; Whitesides, G. E.; Wrighton, M. S. *Science* **1991**, *252*, 688.

(13) (a) Zareie, M. H.; Ma, H.; Reed, B. W.; Jen, A. K.-Y.; Sarikaya, M. *Nano Lett.* **2003**, *3*, 139. (b) Kang, S. H.; Ma, H.; Kang, M.-S.; Kim, K.-S.; Jen, A. K.-Y.; Zareie, M. H.; Sarikaya, M. *Angew. Chem., Int. Ed.* **2004**, *43*, 1512. (c) Poirier, G. E. *Chem. Rev.* **1997**, *97*, 1117.

stirred at 0 °C for 30 min, the solution of potassium iodide (3.98 g, 24.0 mmol) in water (5 mL) was dropwise added. The resulting reaction mixture was stirred at 0 °C for 1 h and then at room temperature for 1 h. The mixture was poured into the solution of K_2CO_3 (23.5 g) in water (500 mL) and $Na_2S_2O_3$ was added to remove I_2. The crude product was collected by filtration and purified by silica gel column chromatography, eluting with hexane/methylene chloride = 1/1 to afford an orange solid (5.10 g, 76%). ^{1}H NMR (300 MHz, $CDCl_3$, TMS): δ 8.20−8.46 (m, 4H), 7.70−7.85 (m, 2H), 7.39 (t, 1H, J = 7.8 Hz). ^{13}C NMR (300 MHz, $CDCl_3$, TMS): δ 187.2, 148.5, 136.7, 135.1, 133.8, 130.1, 129.2, 128.9, 127.4, 98.2. $C_{14}H_7IO_2$: Calcd C 50.33, H 2.11, I 37.98; found C 50.53, H 1.87, I 37.76. ESI-MS (*m*/*z*): Calcd 334.0; found 334.1.

Synthesis of 1-(Trimethylsilylacetylenyl)anthraquinone (5). The mixture of **4** (1.34 g, 4.0 mmol), trimethylsilylacetylene (0.68 mL, 0.47 g, 4.8 mmol), $Pd(PPh_3)_2Cl_2$ (140 mg, 0.20 mmol), and CuI (38 mg, 0.20 mmol) in diisopropylethylamine (10 mL) and dry THF (10 mL) was heated at 40 °C overnight under nitrogen. The solvent in the reaction mixture was evaporated and the crude product was extracted with CH_2Cl_2. The combined organic layers were dried over Na_2SO_4 and concentrated. The residue was separated by silica gel column chromatography, eluting with hexane/methylene chloride = 1/1 to afford an orange solid (1.07 g, 88%). ^{1}H NMR (300 MHz, $CDCl_3$, TMS): δ 8.25−8.35 (m, 2H), 7.95 (dd, 1H, J = 7.8, 0.9 Hz), 7.75−7.85 (m, 2H), 7.70 (t, 2H, J = 7.8 Hz), 0.36 (s, 9H). ^{13}C NMR (300 MHz, $CDCl_3$, TMS): δ 187.3, 143.2, 139.7, 139.3, 135.7, 132.1, 131.6, 129.9, 129.6, 123.8, 85.2, 78.3, −0.7. $C_{19}H_{16}O_2Si$: Calcd C 74.96, H 5.30, Si 9.23; found C 74.77, H 5.15, Si 9.36. ESI-MS (*m*/*z*): calcd 304.1; found 304.0.

Synthesis of 1-Acetylenylanthraquinone (6). To the solution of **5** (1.01 g, 3.3 mmol) in methanol (20 mL) was added K_2CO_3 (0.50 g, 3.6 mmol) and the resulting mixture was stirred overnight at room temperature under nitrogen. The solvent in the reaction mixture was evaporated and the crude product was extracted with CH_2Cl_2. The combined organic layers were dried over Na_2SO_4 and concentrated. The residue was separated by silica gel column chromatography, eluting with methylene chloride to afford a slightly yellow solid (0.63 g, 82%). ^{1}H NMR (300 MHz, $CDCl_3$, TMS): δ 8.25−8.40 (m, 2H), 7.95 (dd, 1H, J = 7.8, 1.2 Hz), 7.70−7.95 (m, 4H), 3.62 (s, 1H). ^{13}C NMR (300 MHz, $CDCl_3$, TMS): δ 187.2, 143.1, 139.6, 139.2, 135.6, 132.1, 131.6, 129.9, 129.7, 123.8, 84.7, 78.5. $C_{16}H_8O_2$: Calcd C 82.75, H 3.47; found C 82.62, H 3.37. ESI-MS (*m*/*z*): Calcd 232.1; found 232.0.

Synthesis of 9-Bromo-10-methylanthracene (8). The solution of 9,10-dibromoanthracene (**7**) (10.08 g, 30.0 mmol) in dry THF (100 mL) was cooled to −78 °C under nitrogen. *n*-Butyllithium (14.4 mL, 2.5 M in hexane, 36.0 mmol) was added dropwise to the solution and allowed to stir for 2 h at −78 °C. Iodomethane (2.4 mL, 5.54 g, 39.0 mmol) was dropwise added and stirred at −78 °C for 2 h. The solution was warmed to room temperature for 1 h and poured into water. The precipitate was collected, washed with H_2O, and dried in a vacuum oven to afford a yellow solid (7.36 g, 91%). ^{1}H NMR (300 MHz, $CDCl_3$, TMS): δ 8.59 (dd, 2H, J = 7.8, 1.5 Hz), 8.30 (dd, 2H, J = 7.8, 1.5 Hz), 7.50−7.65 (m, 4H), 3.09 (s, 3H). ^{13}C NMR (300 MHz, $CDCl_3$, TMS): δ 133.0, 131.8, 127.8, 126.1, 125.6, 125.3, 119.2, 17.7. $C_{15}H_{11}Br$: Calcd C 66.44, H 4.09; found C 66.25, H 3.91. ESI-MS (*m*/*z*): Calcd 270.0; found 270.0.

Synthesis of 9-Iodo-10-methylanthracene (9). A mixture of **8** (1.00 g, 3.7 mmol), copper(I) iodide (3.51 g, 18.5 mmol), potassium iodide (6.49 g, 39.1 mmol), and hexamethylphosphoric triamide (HMPA) (15 mL) is stirred for 6 h at 150−160 °C under nitrogen. The reaction is quenched by the addition of dilute hydrochloric acid (1 N, 40 mL) followed by benzene (40 mL) and the resulting mixture is freed from insoluble copper(I) salts by filtration. The organic phase is separated, washed with water, and evaporated to leave a yellow solid. The crude product was purified by silica gel column chromatography, eluting with methylene chloride to afford a yellow solid (1.04 g, 89%). ^{1}H NMR (300 MHz, $CDCl_3$, TMS): δ 8.55 (dd, 2H, J = 6.2, 1.8 Hz), 8.26 (dd, 2H, J = 6.2, 1.8 Hz), 7.55−7.62 (m, 4H), 3.11 (s, 3H). ^{13}C NMR (300 MHz, $CDCl_3$, TMS): δ 138.9, 134.1, 133.2, 130.5, 126.9, 126.3, 126.0, 96.4, 17.6. $C_{15}H_{11}I$: Calcd C 56.63, H 3.48; found C 56.45, H 3.60. ESI-MS (*m*/*z*): Calcd 318.0; found 318.1.

Synthesis of (10-Methyl-9-anthryl)(1-anthraquinonyl)-acetylene (10). The mixture of **6** (0.23 g, 1.0 mmol), **9** (0.35 g, 1.1 mmol), $Pd(PPh_3)_2Cl_2$ (35 mg, 0.05 mmol), and CuI (9.5 mg, 0.05 mmol) in diisopropylamine (10 mL) was heated at 80 °C overnight under nitrogen. The solvent in the reaction mixture was evaporated and the crude product was extracted with CH_2Cl_2. The combined organic layers were dried over Na_2SO_4 and concentrated. The residue was separated by silica gel column chromatography, eluting with hexane/methylene chloride = 1/1 to 1/2 to afford a red solid (0.37 g, 87%). ^{1}H NMR (300 MHz, $CDCl_3$, TMS): δ 8.26−8.52 (m, 6H), 7.50−7.90 (m, 9H), 3.18 (s, 3H). ^{13}C NMR (300 MHz, $CDCl_3$, TMS): δ 187.2, 143.1, 139.5, 139.2, 135.9, 135.7, 132.3, 132.0, 131.6, 131.2, 130.1, 129.6, 128.3, 126.1, 125.2, 125.0, 123.7, 118.3, 91.2, 17.7. $C_{31}H_{18}O_2$: Calcd C 88.13, H 4.29; found C 88.01, H 4.07. ESI-MS (*m*/*z*): Calcd 422.1; found 422.0.

Synthesis of (10-Acetylthiomethyl-9-anthryl)(1-anthraquinonyl)-acetylene (11). To the solution of **10** (0.34 g, 0.81 mmol) in anhydrous carbon tetrachloride (60 mL) was added *N*-bromosuccimide (NBS) (0.15 g, 0.85 mmol) and benzoylperoxide (BPO) (20 mg, 0.081 mmol). The mixture was refluxed overnight under nitrogen and filtered to remove insoluble succimide side product. The filtrate was concentrated to provide the dry residue followed by the addition of dry THF (30 mL) and potassium thioacetate (93 mg, 0.81 mmol). The reaction mixture was refluxed overnight under nitrogen. The solvent in the reaction mixture was evaporated and the crude product was extracted with CH_2Cl_2. The combined organic layers were dried over Na_2SO_4 and concentrated. The residue was separated by silica gel column chromatography, eluting with hexane/methylene chloride = 1/2 to afford a red solid (0.15 g, 36%). ^{1}H NMR (300 MHz, $CDCl_3$, TMS): δ 8.20−8.46 (m, 6H), 7.78−7.86 (m, 4H), 7.52−7.70 (m, 5H), 5.21 (s, 2H), 3.16 (s, 3H). ^{13}C NMR (300 MHz, $CDCl_3$, TMS): δ 196.7, 187.3, 143.1, 139.5, 139.1, 135.8, 135.6, 132.3, 132.0, 131.6, 131.2, 129.9, 129.7, 128.3, 126.2, 125.3, 125.1, 123.7, 118.3, 91.2, 33.8, 27.8. $C_{33}H_{20}O_3S$: Calcd C 79.82, H 4.06, S 6.46; found C 80.09, H 4.29, S 6.27. ESI-MS (*m*/*z*): Calcd 496.1; found 496.1.

The Preparation and STM Imaging of SAM of 1. Commercial Au(111)/mica film (Molecular Imaging, Inc.) was used as a substrate. It was annealed at 350 °C for 6 h in a furnace before use and then cut into sections, washed with ethanol, and dried under a stream of high-purity argon immediately. The solution of **11** (50 μM) in ethanol (absolute, 200 proof) was prepared and bubbled with nitrogen and ammonium hydroxide (1.0 μL (28.0−30.0% NH_3) per mL of solution) was added. Then gold substrates were immediately immersed into the solution for 24 h, followed by rinsing with ethanol and drying with a nitrogen stream. STM tips were prepared by mechanically cutting a Pt/Ir (80/20) wire (0.25 mm in diameter). The STM experiment was performed on Nanoscope III SPM (Digital Instruments, Santa Barbara, CA). All STM images shown here were collected in the constant-current mode under ambient conditions at room temperatures.

Electrochemical and Photoelectrochemical Measurements. All electrochemical studies were performed on a Bioanalytical Systems, Inc. CV-50W voltammetric analyzer using a three-electrode cell

Scheme 1. Synthesis of Self-assembling Molecule with Coplanar Anthraquinonyl and Anthryl Moieties

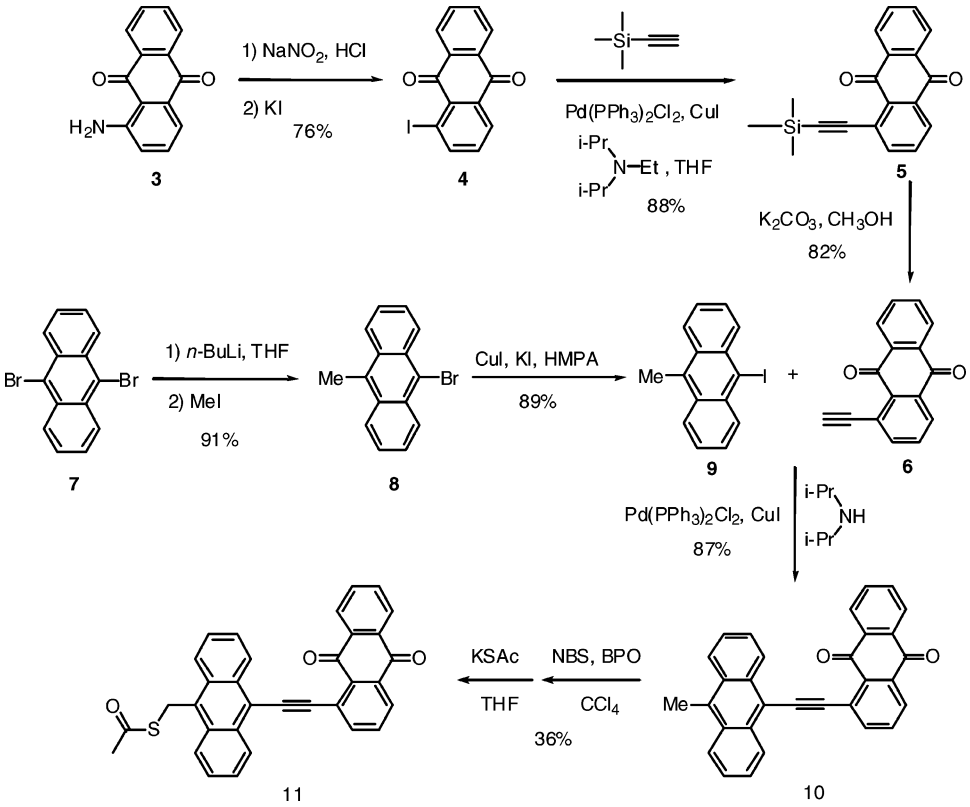

with a SAM-modified Au working electrode, platinum foil counter electrode, and a Ag/AgCl reference. SAMs on the gold were characterized to confirm the surface-confinement using cyclic voltammetry at scan rates ranging from 100 to 500 mV/s in the presence of tetrabutylammonium hexafluorophosphate (Bu_4NPF_6) dissolved in acetonitrile. Photoelectrochemical measurements were carried out in a one-compartment cell. The SAM-modified working electrode was illuminated with monochromatic excitation light of a certain wavelength through a monochromator in 0.1 M Na_2SO_4 aqueous solution containing 50 mM MV^{2+} as an electron carrier. The light intensity was monitored by a Multi-Function Optical Meter (Newport, Model 2835-C). Quantum yield (ϕ) of photocurrent generation of the [Au/SAM/MV^{2+}/Pt] cell was calculated by the following equation: $\phi = (i/e)/[I(1-10^{-A})]$, where $I = (W\lambda)/(hc)$, i is the photocurrent density, e is the elementary charge, I is the number of photons per unit area and unit time, λ is the wavelength of light irradiated, A is absorbance of the absorbed chromophores at λ, W is light power irradiated at λ, c is the light velocity, and h is the Planck constant. Absorbance (A) of the adsorbed chromophores at λ was calculated by assuming that the absorption coefficient of chromophore on a gold substrate is the same as that in solution.

Results and Discussion

The synthetic procedure for making the acetyl protected target molecule **1** (compound **11**) is outlined in Scheme 1. The synthesis of **11** was accomplished through the Sonogashira coupling reaction between 9-iodo-10-methylanthracene (**9**) and 1-anthraquinonyl acetylene (**6**) followed by bromination of the benzylic group on **10** and the subsequent nucleophilic substitution with potassium thioacetate. The intermediate **9** was prepared via the monolithiation of 9,10-dibromoanthracene (**7**) with *n*-butyllithium at −78 °C and then quenching of the resulting anion with iodomethane to generate 9-bromo-10-methylanthracene (**8**) and then through the copper(I) iodide-mediated halogen exchange with iodide ion in hot hexamethylphosphoric triamide (HMPA). The other intermediate **6** was synthesized from 1-aminoanthraquinone (**3**) via the diazotization-Sandmeyer reaction to afford 1-iodo-anthraquinone (**4**) followed by the Sonogashira coupling with trimethylsilylacetylene and then the base-catalyzed desilylation.

The SAM derived from molecule **1** was prepared by immersing Au(111)/mica substrate in a solution of **11** in EtOH at 25 °C for 24 h in the presence of ammonium hydroxide to hydrolyze the acetyl protecting group. The result from high-resolution scanning tunneling microscopy (STM) images recorded at room temperature confirms that the SAM of **1** forms a well-ordered 2D nanostructure. Figures 2a and 2b show a top view and a height-shaded surface plot, respectively. A low-pass filtered transform was employed to remove the scanning noise in the STM images. It can be seen from Figure 2a that the SAM consists of ordered bright spots with elongated features, corresponding to the individual molecules of **1**. The length of each bright spot is measured to be 0.89 ± 0.20 nm, which is very close to the calculated width of molecule **1**, which indicates that these molecules stand on the Au(111) substrate through Au−S bonding. According to previous studies on self-assembly of thiols on Au(111), sulfur atoms occupy the hollow sites with lower energy compared to the bridge or top sites of Au(111).[13c] The intermolecular distance along the **A** direction is measured to be 0.61 ± 0.20 nm, which is close to 2 times that of the Au(111) lattice parameter (0.288 nm). The intermolecular distance along the **B** direction is measured to be 0.78 ± 0.20 nm, which corresponds to $\sqrt{7}$ times that of the

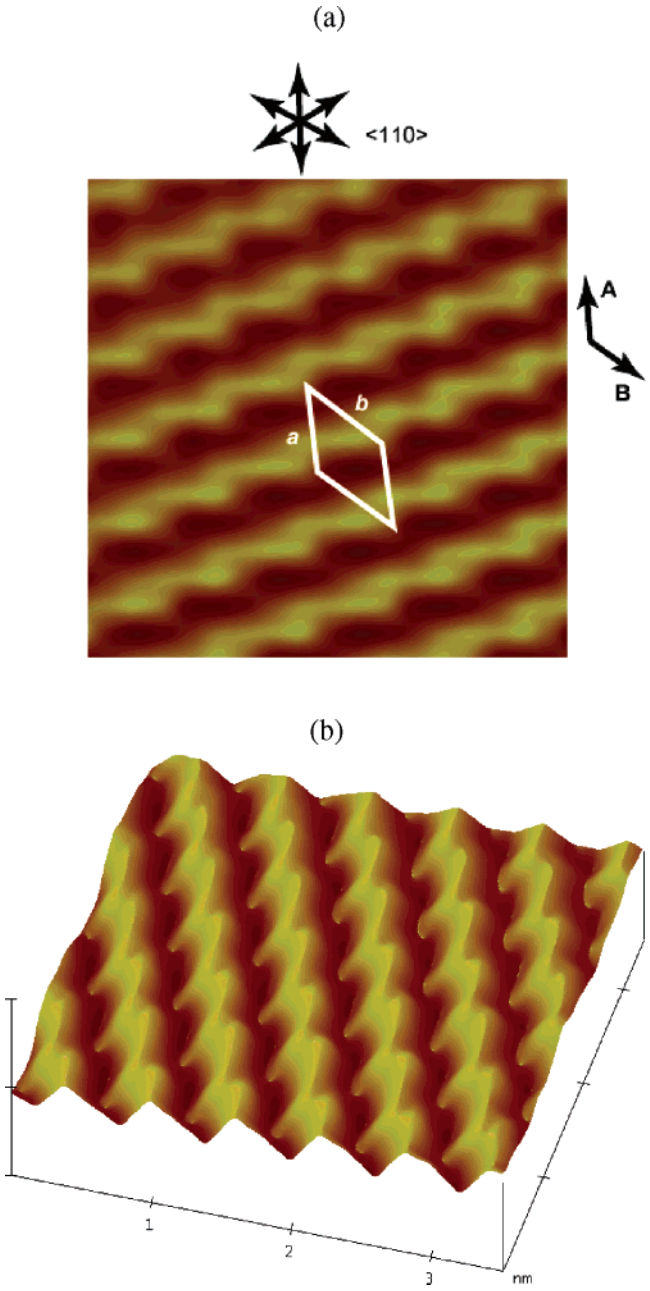

Figure 2. High-resolution STM images of ordered assemblies of electron acceptor molecule **1** on Au(111) at room temperature. (a) Top-view; (b) height-shaded surface plot. Scan size is 3.5 nm × 3.5 nm. Setpoint was 500 pA, and bias was 200 mV.

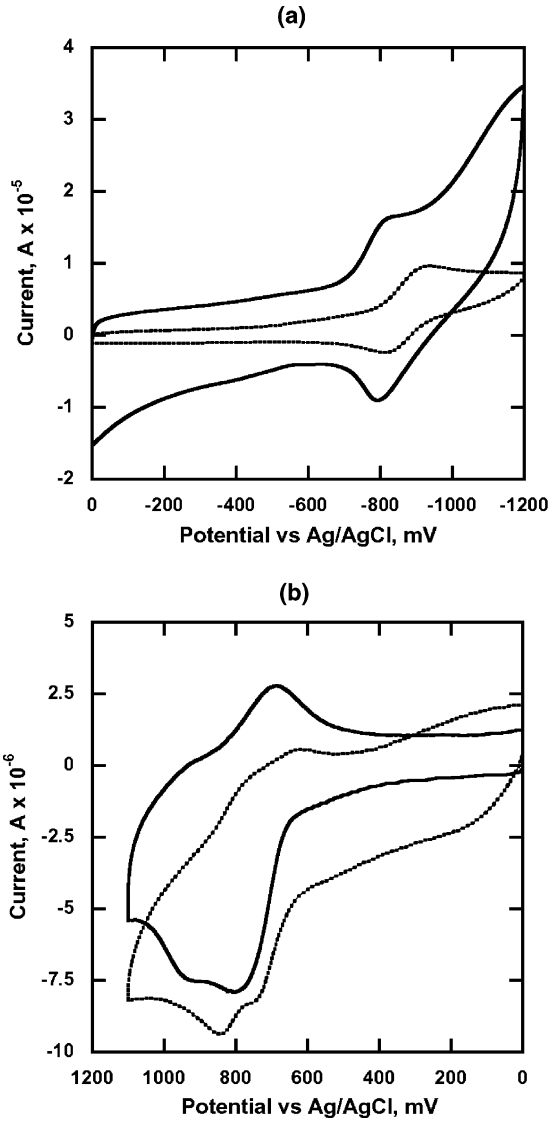

Figure 3. Cyclic voltammograms of (a) electron acceptor **1** in solution (dotted line) and its SAM on gold (solid line); (b) electron donor **2** in solution (dotted line) and its SAM on gold (solid line). Cyclic voltammograms were carried out in acetonitrile containing 0.1 M Bu_4NPF_6 as a supporting electrolyte at a sweep rate of 100 mV/s.

Au(111) lattice parameter. The angle between the two directions is 42° ± 2°. Based on the intermolecular distance and orientation of molecular rows, a (2 × $\sqrt{7}$) adlayer structure for the SAM of **1** on Au(111) can be determined. A unit cell is outlined in Figure 2a. From the STM images, it can be clearly discerned that adsorbed molecules on Au(111) form a close stack with one another, similar to the interplanar stacking of graphite, with an interplanar spacing of 0.31 ± 0.04 nm (compared to 0.34 nm for graphite). It can be attributed to the strong intermolecular $\pi-\pi$ stacking derived from the coplanar fused rings of anthraquinone and anthrathene. The overall well-ordered and unique molecular arrangements in the SAM of **1** may also arise from a delicate interplay between the intermolecular interactions dominated by the strong intermolecular $\pi-\pi$ stacking, involving both steric hindrance and weak dipole−dipole interactions, and Au−S bonding between the molecules and Au(111) substrate, where the latter appears to play a secondary role.

The electrochemical behavior of molecules **1** and **2** as well as their SAMs on Au was evaluated by using cyclic voltammetry (CV) performed in acetonitrile containing 0.1 M of *n*-Bu_4NPF_6 as electrolyte and swept at a rate of 100 mV/s. The CVs of **1** and its SAM on Au showed reversible characteristics (Figure 3a) which have peak splitting of 120 and 30 mV, and $E_{1/2}$'s of −0.87 and −0.81 V vs Ag/AgCl, respectively. The small peak-to-peak separation (30 mV) suggests rapid electron-transfer reaction kinetics for the SAM of **1** on Au. To construct two-component mixed SAMs for photocurrent generation efficiency studies, it is crucial to have a donor molecule that can be paired with molecule **1** for co-assembly. The molecule **2** (Figure 1) was designed to have an oligo(pyrrolethiophene) unit with lower oxidation potential than that of oligo(thiophenes),[14] and it has two fully π-conjugated, rigid,

Table 1. Dependence of Surface Coverage on Feeding Molar Ratios

molar ratio in solution (**2**:**1**)	surface coverage (10^{-10} mol/cm^2) **2**	**1**	molar ratio in mixed SAMs[a] (**2**:**1**)
0:1	0	4.8	0:1
1:10	1.0	4.2	0.24:1
1:1	2.2	2.8	0.8:1
10:1	2.5	1.3	1.9:1
20:1	2.8	0.9	3.1:1
1:0	2.9	0	1:0

[a] Molar ratios of **2** to **1** in the mixed SAMs on the gold substrate were determined from electrochemical measurements.

footing thiols for better affinity to gold surface compared to the molecules with only a monothiol. The detailed synthesis and SAM characteristics of **2** will be reported elsewhere. ^{1}H NMR, elemental analysis, and low-resolution mass spectral data for compound **2** are summarized in the Supporting Information. The redox behavior of molecule **2** and its SAM on gold are shown in Figure 3b. Two redox waves of **2** in solution and its SAM on gold were observed, but corresponding cathodic waves were not as clear as those anodic waves due to instability of the radical anion produced by the reduction. Redox potentials ($E_{1/2}$ vs Ag/AgCl) and peak splittings of **2** in solution and in SAM were observed to be 0.67 and 0.74 V and 100 and 120 mV from its first oxidation step, respectively.

The amounts of adsorbed electron acceptor **1** and electron donor **2** in their homo- and co-assemblies on gold were calculated from the charge of cathodic or anodic peaks of the molecules (Table 1). The surface coverage of a homo-SAM of **1** calculated from the CV peak (4.8×10^{-10} mol/cm^2) is very close to that calculated from the STM image (5.0×10^{-10} mol/cm^2). It should be noted that the surface coverage (2.9×10^{-10} mol/cm^2) of **2** in the homo-SAM is very different from that of **1** due to the different molecular dimensions and structures, i.e., extended π-conjugation and coplanarity, which can affect intermolecular interactions and packing density of SAMs. The higher surface coverage of **1** in the homo-SAM may be due to more thermodynamically favorable packing than that of **2**, due to strong intermolecular $\pi-\pi$ stacking and small molecular dimension. Since molecule **2** does not take part in the reduction reaction and molecule **1** does not take part in the oxidation reaction of the SAMs on gold within the scanning potential range, it can be assumed that, in the CVs of mixed SAMs, the oxidation peak is derived from molecule **2** and the reduction peak is derived from molecule **1**. The amounts of each of the self-assembled molecules on gold were systematically changed by the competitive coadsorption onto gold surface from the solutions containing various feeding molar ratios of **1** and **2**. The surface coverage of the mixed SAMs were also calculated and listed in Table 1. As expected, the surface coverage of **2** in the mixed SAMs became higher with the increased feeding ratio of **2** in solution, while the surface coverage of **1** was smaller with the decreased feeding ratio

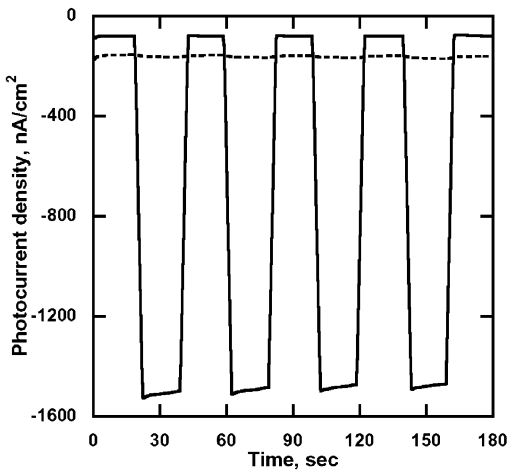

Figure 4. Photoelectrochemical response of homo-SAM of electron acceptor **1** (dotted line) and mixed SAM of **2** and **1** with a feeding molar ratio of 10:1 (solid line) on gold under illumination at 360 nm; electrolyte solution: 0.1 M Na_2SO_4 solution containing 50 mM methyl viologen (MV^{2+}) as an electron carrier; input power: 0.85 W/cm^2; applied potential: -100 mV vs Ag/AgCl.

of **1** in the solution. However, the molar ratio of **1** and **2** in the mixed SAMs do not match well with the original feeding molar ratio in the solution. The final composition of **1** and **2** in the mixed SAMs may be affected by the complicated kinetic and thermodynamic factors during the self-assembly in addition to the different concentrations of components in the feeding solution.

The photoelectrochemical measurements were performed using the pre-assembled mixed SAMs of **1** and **2** on a gold electrode in a 0.1 M Na_2SO_4 aqueous solution containing 50 mM methyl viologen (MV^{2+}) as an electron carrier. The mixed SAM of **1** and **2** on gold was used as the working electrode, along with a platinum counter electrode and a Ag/AgCl reference electrode in a three-electrode configuration. The photocurrent was generated immediately when a monochromatic light source (360 nm) was used to illuminate the mixed SAMs in electrolyte and the initial value of photocurrent went down instantly when the illumination was terminated. As shown in Figure 4, photocurrent responses were recorded under the illumination of a monochromatic wavelength of 360 nm with 0.85 mW/cm^2 light intensity. When Au/**2**:**1** (feeding molar ratio of 10:1)/MV^{2+}/Pt was photoirradiated under a bias voltage of -100 mV/s vs Ag/AgCl, a stable cathodic photocurrent (ca. 1425 nA/cm^2) was generated via intermolecular electron transfer from donor **2** to acceptor **1**, whereas only **1** on gold electrode showed very small photocurrent generation (less than 20 nA/cm) under the same illumination. The amount of generated photocurrent (1425 nA/cm^2) for Au/**2**:**1** (feeding molar ratio of 10:1)/MV^{2+}/Pt is comparable to the result (1700 nA/cm^2) for Au/**2**:C_{60}-anthrylphenylacetylene-thiol[13b] (feeding molar ratio of 10:1)/MV^{2+}/Pt using C_{60} as an electron acceptor. It can be seen that the mixed SAM system using anthraquinone-anthrylacetylene-thiol linked molecule **1** as an electron acceptor is quite promising to mimic the photosynthetic electron transfer of Mother Nature.

The photocurrent generation was also investigated by varying the bias voltage to determine the direction of the

(14) (a) Beckers, E. H. A.; Hal, P. A.; Dhanabalan, A.; Meskers, S. C. J.; Knol, J.; Hummelen, J. C.; Janssen, R. A. J. *J. Phys. Chem. A* **2003**, *107*, 6218. (b) Ferraris, J. P.; Newton, M. D. *Polymer* **1992**, *33*, 391.

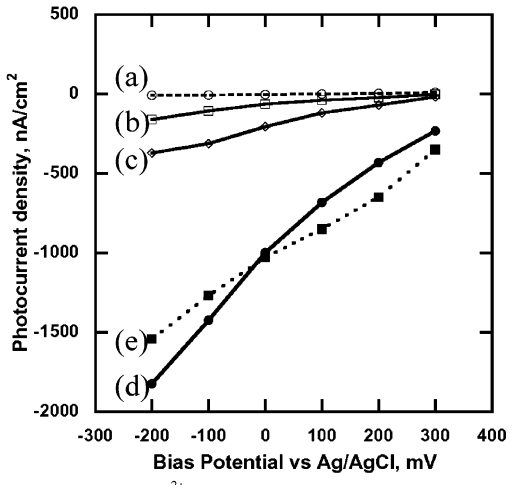

Figure 5. Photocurrent vs bias potential as a function of molar ratio of **2**:**1**; (a) 0:1; (b) 1:10; (c) 1:1; (d) 10:1; (e) 20:1; monochromic wavelength of 360 nm; electrolyte solution: 0.1 M Na_2SO_4 solution containing 50 mM methyl viologen (MV^{2+}) as an electron carrier; input power: 0.85 W/cm^2.

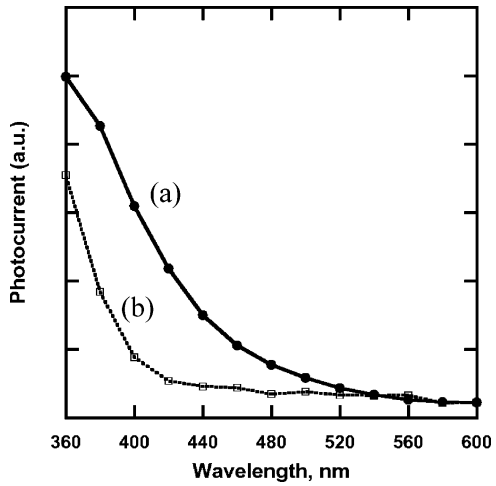

Figure 6. (a) Action spectrum of mixed SAM and (b) UV/vis spectrum of mixed solution with the feeding molar ratio of 10:1 (**2**:**1**) (in toluene); electrolyte solution: 0.1 M Na_2SO_4 solution containing 50 mM methyl viologen (MV^{2+}) as an electron carrier; input power: 0.85 W/cm^2; applied potential: −100 mV vs Ag/AgCl.

current flow. Figure 5 showed the photocurrent generation in mixed SAMs upon the application of different bias potentials to the electrode. The cathodic photocurrent increases dramatically when the bias potential was applied in the range from 300 to −200 mV vs Ag/AgCl. The extent of change in photocurrent was larger when the feeding ratio of electron donor **2** was increased in the solution. The **2**:**1** mixed SAM of molecule with a feeding molar ratio of 10:1 showed the fastest increase in photocurrent response as a function of the bias potential. It is considered that intermolecular electron transfer in the mixed SAM of **2** and **1** (feeding molar ratio of 10:1) is more effective than those of different molar ratios. As purple bacteria,[15] green bacteria,[16] or cyanobacteria[17] have their own organized structures of molecular assemblies to realize highly efficient light harvesting and photosynthesis, the optimized molecular arrangements for light absorption and electron transfer may be achieved in the mixed SAM of this pair of electron donor **2** and electron acceptor **1** with a feeding molar ratio of 10:1. The detailed feature of mixed SAMs is under investigation. The attempt to generate photocurrent with a negative bias of more than −300 mV applied to the gold electrode could not be realized due to the significant increase of the cathodic dark current. A semilinear relationship between cathodic photocurrent vs bias potential in the presence of MV^{2+} was found; the cathodic photocurrent increased as the bias applied to the gold electrode decreased from +300 to −200 mV vs Ag/AgCl under the illumination of 360 nm light, demonstrating that the photocurrent flows from the gold electrode to the counter electrode through the SAM and the electrolyte. Based on its dependency on the applied bias, the photocurrent generation mechanism can be considered as follows: the photoexcitation of molecule **2** in the mixed SAMs induces intermolecular electron transfer from **2** to **1** followed by electron transfer to the redox-species ($MV^{2+}/MV^{+\bullet}$), and then the electrons are transported from $MV^{+\bullet}$ to the counter electrode (Pt), resulting in the observed cathodic photocurrent. Under a negative bias, the holes generated flow toward Au substrate to further generate cathodic photocurrent.

The action spectra of the mixed SAMs were recorded in terms of wavelength with varying molar ratios. The action spectrum of Au/**2**:**1** (feeding molar ratio of 10:1)/MV^{2+}/Pt showed a good agreement with the absorption spectrum of the mixed solution of **2** and **1** (Figure 6). When the excitation wavelengths were varied within the range 360−600 nm, a maximum photocurrent was observed at 360 nm, which is close to the absorption maximum in the range of investigated wavelength.

The quantum yields were determined in terms of the feeding molar ratio by using photocurrent density, absorbance of the SAM on the electrode, and input power at the applied potential. Assuming that the absorption coefficient of **2** in a mixed SAM on gold is the same as that in solution ($\epsilon = 2.2 \times 10^4$ M^{-1} cm^{-1} at 360 nm), the absorbance of **2** in the mixed SAMs on gold with the feeding molar ratio of 10:1 (**2**:**1**) was calculated to be 1.1×10^{-2} at 360 nm. The quantum yield was calculated based on the assumption that the major photon absorber is electron donor **2**, not electron acceptor **1**, since the molecule **2** strongly absorbs photons at 360 nm, based on the UV spectrum. The larger quantum yields were achieved by increasing the molar ratio of **2** to **1** until reaching the highest quantum yield value at the ratio of 10:1. To compare our result to the reported ones in the literature, we calculated the quantum yields of the observed cathodic photocurrent at −100 mV. The quantum yield of photocurrent generation for the mixed SAM with the feeding molar ratio of 10:1 (**2**:**1**) was determined to be 23.1% at −100 mV vs Ag/AgCl with a monochromatic wavelength of 360 nm. The quantum yields for mixed SAMs with molar ratios of 1:10, 1:1, 10:1, and 20:1 (**2**:**1**) were 4.2, 5.5, 23.1, and 18.9%, respectively. It should be noted that this value

(15) (a) Roszak, A. W.; Howard, T. D.; Southall, J.; Gardiner, A. T.; Law, C. J.; Isaacs, N. W.; Cogdell, R. J. *Science* **2003**, *302*, 1969. (b) van Oijen, A. M.; Ketelaars, M.; Khler, J.; Aartsma, T. J.; Schmidt, J. *Science* **1999**, *285*, 400.
(16) Olson, J. M. *Photochem. Photobiol.* **1998**, *67*, 61.
(17) (a) Ferreira, K. N.; Iverson, T. M.; Maghlaoui, K.; Barber, J.; Iwata, S. *Science* **2004**, *303*, 183. (b) Shem, A. B.; Frolow, F.; Nelson, N. *Nature* **2003**, *426*, 630.

of quantum yield for the mixed SAM of **2** and **1** at the molar ratio of 10:1 is much larger than those in similar photoelectrochemical cells using mixed SAMs of porphyrin and alkanethiol (0.26%),[18] C_{60}-linked alkanethiol SAMs (7.5%),[19] and C_{60}-based LB film cells (1.2−8.2%).[20] The value obtained here is smaller than that of the mixed SAMs (as high as 50 ± 8% in quantum yield) reported by Imahori et al.,[9c] but ferrocene-porphyrin-C_{60} triad and boron-dipyrrin light-harvesting molecule were used in that system.

Conclusion

A novel self-assembling molecule with coplanar anthraquinonyl and anthryl moieties has been designed and synthesized as electron acceptors for efficient photocurrent generation. The SAM of this acceptor molecule exhibits highly ordered 2D arrays that form an oblique lattice and graphite-like stacking at room temperature. The co-assemblies based on this acceptor molecule show interesting electrochemical and photoelectrochemical properties. The anthraquinone-anthrylacetylene-thiol linked molecule as an electron acceptor is promising to construct an efficient monochromatic light-to-current molecular converter.

Acknowledgment. This work was supported by the Air Force Office of Scientific Research (AFOSR) under the Bioinspired Concept Program and the Army Research Office (ARO) under the DURINT Program. Alex K.-Y. Jen thanks the Boeing-Johnson Foundation for its support.

Supporting Information Available: Additional experimental details and figures (PDF). This material is available free of charge via the Internet at http://pubs.acs.org.

CM050243W

(18) Imahori, H.; Hasobe, T.; Yamada, H.; Nishimura, Y.; Yamazaki, I.; Fukuzumi, S. *Langmuir* **2001**, *17*, 4925.
(19) Imahori, H.; Azuma, T.; Ajavakom, A.; Norieda, H.; Yamada, H.; Sakata, Y. *J. Phys. Chem. B* **1999**, *103*, 7233.
(20) Luo, C.; Huang, C.; Gan, L.; Zhou, D.; Xia, W.; Zhuang, Q.; Zhao, Y.; Huang, Y. *J. Phys. Chem*. **1996**, *100*, 16685.